# INTERNATIONAL SOCIETY FOR SOIL MECHANICS AND GEOTECHNICAL ENGINEERING



This paper was downloaded from the Online Library of the International Society for Soil Mechanics and Geotechnical Engineering (ISSMGE). The library is available here:

## https://www.issmge.org/publications/online-library

This is an open-access database that archives thousands of papers published under the Auspices of the ISSMGE and maintained by the Innovation and Development Committee of ISSMGE.

The paper was published in the proceedings of the 20<sup>th</sup> International Conference on Soil Mechanics and Geotechnical Engineering and was edited by Mizanur Rahman and Mark Jaksa. The conference was held from May 1<sup>st</sup> to May 5<sup>th</sup> 2022 in Sydney, Australia.

## Numerical study on seismic performance of high mudstone embankment against two types of seismic wave

Étude numérique sur les performances sismiques des hauts remblais de mudstone contre deux types d'ondes sismiques

### Shogo INUKAI & Masaki NAKANO

Civil Engineering, Nagoya University, Japan, inukai.syogo@i.mbox.nagoya-u.ac.jp

ABSTRACT: The reduced stability of mudstone embankments due to slaking is a severe problem. In this study, a ground survey was carried out on a mudstone embankment. Based on the result, a soil—water coupled finite deformation analysis for the embankment was conducted to grasp the seismic behavior and to assess the seismic performance of the embankment under two types of seismic wave with different properties. The following are new findings. 1) The triaxial compression test results were simulated by an elastoplastic constitutive model considering the sampling process, and the test results could be reproduced. This confirmed that the analysis model was valid. 2) When data from the Great East Japan Earthquake were input, the mean effective stress of the embankment was reduced by a long seismic wave, and then the shear strain progressed. However, data from the Hyogo-ken Nanbu Earthquake did not lead to large deformation because the seismic duration was short. 3) The slaking ratio was changed because of the fluctuation of the underground water level over many years. Therefore, the slaking ratio is not a value inherent to the mudstone.

RÉSUMÉ: Le fait que la stabilité d'un remblai de mudstone soit réduite par la battance est un problème grave. Dans cette étude, nous avons effectué un relevé de terrain sur un remblai de mudstone. À partir des résultats, nous avons réalisé une analyse de déformation finie couplée sol-eau pour le remblai afin de comprendre le comportement sismique du remblai et en évaluer les performances sismiques. Les nouvelles découvertes sont les suivantes. 1) Les résultats du test de compression triaxiale ont été simulés par un modèle constitutif élasto-plastique qui prend en compte le processus d'échantillonnage, et les résultats du test ont pu être reproduits. 2) Lors de la saisie du séisme de la côte Pacifique du Tohoku, la contrainte effective moyenne sur le remblai a été réduite par une longue onde sismique, puis la déformation de cisaillement a progressé. En revanche, le tremblement de terre de Kanbu (Hyogo-ken) n'a pas causé de grandes déformations car le séisme fut de courte durée. 3) Le rapport de battance a changé en raison des fluctuations de niveau des eaux souterraines sur plusieurs années. Par conséquent, le rapport de battance n'est pas une valeur inhérente à la mudstone.

KEYWORDS: mudstone, embankment, seismic response analysis

## 1 INTRODUCTION

It is important to ensure the seismic resistance of expressways, which can function as emergency transportation routes. In particular, the embankment must resist huge seismic events, such as the Nankai Trough Earthquake, which is expected to occur in the near future. However, the Tertiary mudstone distributed throughout Japan has often been used for expressways, and some mudstone becomes muddy because of rainfall and groundwater. This is called the "slaking phenomenon". In previous studies, laboratory tests on crushed mudstone aggregate samples have confirmed a decrease in strength resulting from repeated dry and wet conditions. It was also indicated that slaking was one of the causes of embankment collapse near the Tomei Expressway Makinohara SA that occurred in 2009 caused by an earthquake with a seismic center off Suruga Bay. Nakano et al. (2016) expressed the slaking phenomenon of mudstone by the concept of the soil skeleton structure and reproduced the embankment collapse by GEOASIA (Noda et al. (2008)), which is a soil–water coupled finite deformation analysis code. As a result, they showed that the decrease in strength due to slaking at the bottom of the embankment was the cause of the collapse.

The purpose of this study was to understand the seismic behavior of a high mudstone embankment based on detailed ground surveys, such as boring, sampling, and laboratory tests. Numerical analysis was performed using *GEOASIA* equipped with SYS Cam-clay model.

## 2 FEATURES AND LAYER CLASSIFICATION OF TARGET EMBANKMENT

Fig. 1 shows a cross section of the embankment used in the analysis. The embankment was on inclined ground and was approximately 30 m in height. The ground survey was carried out around 20 years later from construction of embankment. The boring positions at the four points are shown in Fig. 1 (Bor. 1 to Bor. 4). In addition, the highest and lowest groundwater levels during the survey period were observed using a self-recording water level gauge. Because a mountain stream exists near the embankment, the groundwater level is high at Bor. 4 on the upstream side, and it is low from Bor. 2 on the downstream side to Bor. 3 at the toe of the slope. Therefore, groundwater flows from the upper part of the embankment toward the toe constantly. The slaking ratio test (JHS) at the time of construction was as low as 6.6% to 15.2%. However, the test at the time of the survey 14 years later was 73.9%, which was remarkably different from the result at the time of construction. Assuming the same mudstone, the result implied that, even though the mudstone had a low slaking ratio at the time of construction, the ratio changed because of the fluctuation of the underground water level over many years. Therefore, the slaking ratio is not a value inherent to the mudstone.

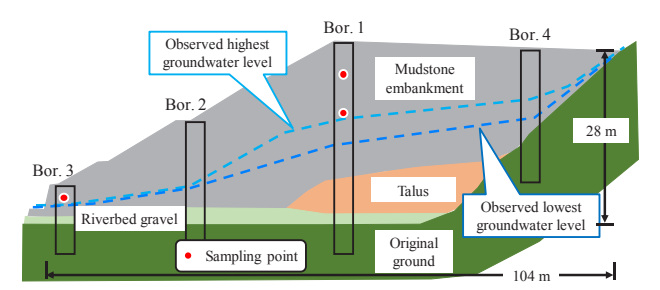


Figure 1. Embankment cross section

Fig. 2 shows the N value and grain size of Bor. 1 with depth. The gravel content was 60% or more from the ground surface to a depth of 10 m, while it was almost 50% or less at below the observed highest groundwater level near a depth of 12 m. However, the clay content was high below the observation groundwater level.

Here, the gravel was mainly crushed mudstone of a large grain size, and the gravel was undergoing grain refining below the groundwater level. In addition, the N value near the ground surface was approximately 10. However, it exceeded 50 near a depth of 10 m with a large amount of gravel, and it was approximately 20 below the groundwater level. In addition to these differences in physical properties, considering that different embankment materials were used from the surface to a depth of approximately 6 m, the mudstone embankment was divided into three layers, as shown at the right side of Fig. 2. Hereinafter, the embankment materials used in this analysis are referred to as Layer 1, Layer 2, and Layer 3.

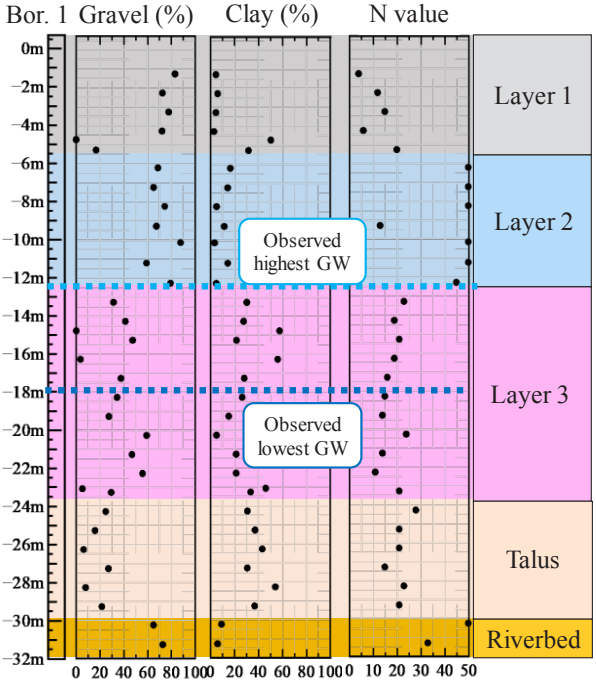


Figure 2. Physical properties obtained by boring survey

### 3 ANALYSIS CONDITIONS AND PROCEDURES

The numerical analysis included approximately 15 years of data until the ground survey, considering the embankment construction process. Then, the two types of seismic wave were input, and the behavior of the embankment during each earthquake was examined.

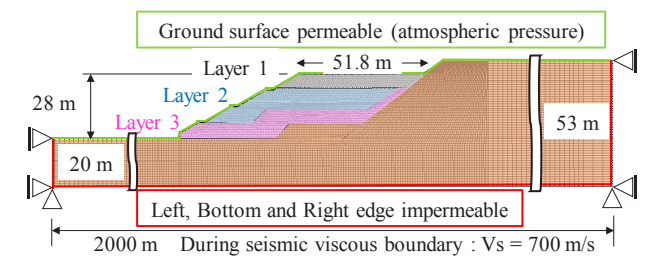


Figure 3. Finite element after embankment construction and boundary conditions

Table 1. Initial states and material constants of the embankment

Table 1. Initial states and material constants of the embankment				
Material name		Layer 1	Layer 2	Layer 3
Parameters for elastoplasticity				
Compression index	$\widetilde{\lambda}$	0.085	0.080	0.080
Swelling index	$\widetilde{\kappa}$	0.015	0.018	0.018
Critical state constant	M	1.375	1.350	1.350
Intercept of NCL	N	1.350	1.380	1.380
Poisson's ratio	$\nu$	0.300	0.150	0.150
Parameters for evolution law				
Degradation index of overconsolidation	m	0.200	0.300	0.300
Degradation index of structure ( $b = c = 1$ )	а	0.400	0.500	0.500
Plasticity index	$C_S$	0.100	0.100	0.100
Rotational hardening index	$b_r$	0.010	0.010	0.010
Limitation of rotational hardening	$m_b$	1.000	1.000	1.000
Physical properties				
Coefficient of permeability (cm/s)	k	$10^{-7}$	$10^{-4}$	$10^{-7}$
Soil density (g/cm <sup>3</sup> )	$ ho_{ m s}$	2.658	2.657	2.657
Initial state values				
Specific volume	$\mathbf{v}_0$	1.453	1.420	1.504
Structure	$1/R^*_0$	10.0	14.4	45.0
Anisotropy	$\zeta_0$	0.000	0.000	0.000
Stress ratio	$\eta_0$	0.100	0.150	0.160

This analysis used GEOASIA, which is a soil-water coupled finite deformation analysis code. Fig. 3 shows the finite-element mesh after embankment construction and the boundary conditions. This analysis was carried out under plane-strain conditions. The width of the analysis area was set to 2000 m, which was enough width, so that both ends of the analysis area did not affect the analysis results. It was assumed that both the embankment and the basement were saturated, and a viscous boundary (Vs = 700 m/s) was given in the horizontal direction of the bottom edge during earthquakes. The embankment part was divided into three layers, as shown in Section 2, while the basement consisted of riverbed gravel, talus, and original ground. To determine the material constants for each layer of the embankment, laboratory tests were carried out using undisturbed samples from Bor. 1 for Layers 1 and 2 and from Bor. 3 for Layer 3, and the results were simulated using the SYS Cam-clay model. The sampling positions are shown in Fig. 1. The material constants of the soil in Layers 2 and 3 were set to the same value because the mechanical behaviors for the remolded samples of Layers 2 and 3 were almost the same. The initial state values were also obtained by simulating the shear behavior considering the stress path for the process from the embankment construction to the sampling. The material constants of the basement were assumed to be the same as that of Layer 2, and the initial specific

volume was small to avoid deformation during earthquakes. Table 1 shows the initial state values and material constants obtained from the reproduction results.

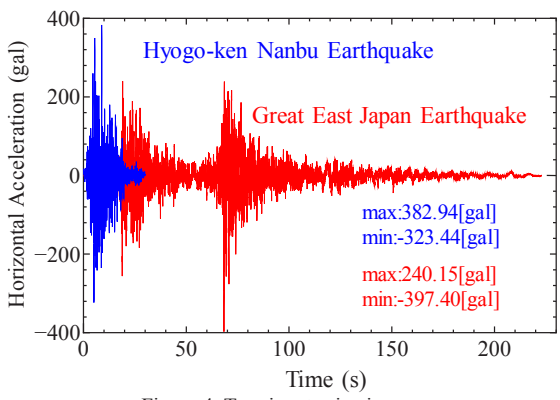


Figure 4. Two input seismic waves

Fig. 4 shows the two input seismic waves used in this numerical analysis. The blue line is the seismic wave of Hyogoken Nanbu Earthquake, Level-2. The seismic duration is 30 s. The red line is the seismic wave of the Great East Japan Earthquake, Level-2. The seismic duration is 223 s. It is also characterized by having the two large acceleration groups.

## 4 SIMULATION RESULTS: VALIDATION OF ANALYSIS CODE AND MATERIAL CONSTANTS

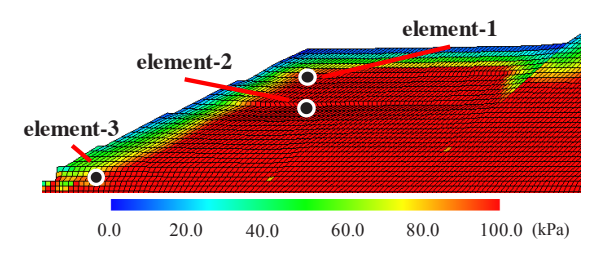


Figure 5. Distribution of mean effective stress at the time of the ground survey

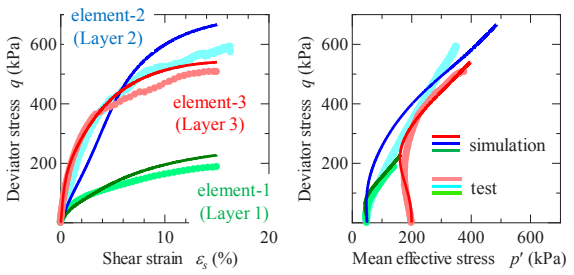


Figure 6. Comparison of the triaxial test results and analysis results

The validity of this analysis code and the set material constants was confirmed. First, using the material constants shown in Table 1, the analysis was performed considering the embankment construction process. The earthquake occurred near the analysis target during the service. The analysis was conducted for the earthquake and continued until the time of the ground survey. Fig. 5 shows the distribution of the mean effective stress at the time of the ground survey. The soil elements of Layer 1 (element-1), Layer 2 (element-2), and Layer 3 (element-3) indicate the sampling positions of the undisturbed sample that were subjected to a triaxial test. Fig. 6 shows a comparison of the triaxial test results and analysis results for undisturbed samples in each soil element. The results of the triaxial test could be reproduced in all layers. Therefore, the state inside the embankment at the time of the ground survey could be simulated. It was confirmed that the

analysis code, estimated initial states, and material constants were valid

## 5 SIMULATION RESULTS: SEISMIC BEHAVIOR OF THE EMBANKMENT DURING EACH EARTHQUAKE

#### 5.1 Hyogo-ken Nanbu Earthquake

Fig. 7 shows the shear strain distribution at the end of the earthquake. As shown in the figure, although a large deformation did not occur, the shear strain at the bottom of the embankment and the toe of the slope occurred at approximately 25%.

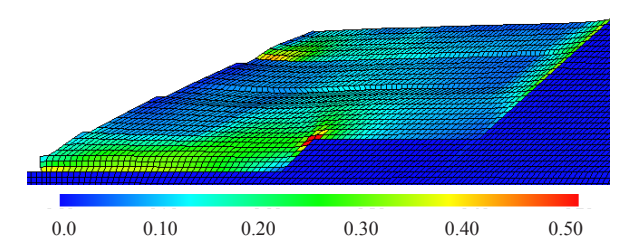


Figure 7. Shear strain distribution at the end of the earthquake

### 5.2 Great East Japan Earthquake

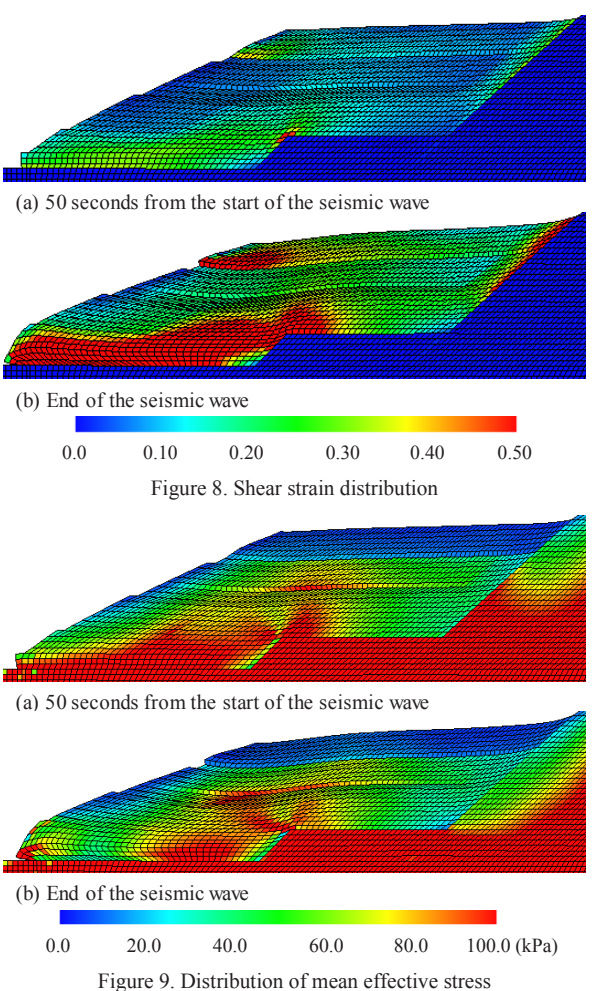


Fig. 8 shows the shear strain distribution, and Fig. 9 shows the distribution of mean effective stress. The figures show (a) 50 s from the start of the seismic wave, which was the first acceleration group input, and (b) the end of the seismic wave. Fig. 8 (a) indicated that shear strain occurred at the bottom of the embankment and the toe of the slope, but large shear strain did not occur in the first acceleration group. However, the mean

effective stress in Fig.8(a) was low compared with Fig. 5 (before the seismic wave), and therefore large shear strain progressed at the bottom of the embankment and the toe of the slope, and large deformation occurred, as shown in Fig. 8 (b), during the second acceleration group.

## 5.3 Determining the behavior of the toe of the slope during each seismic wave

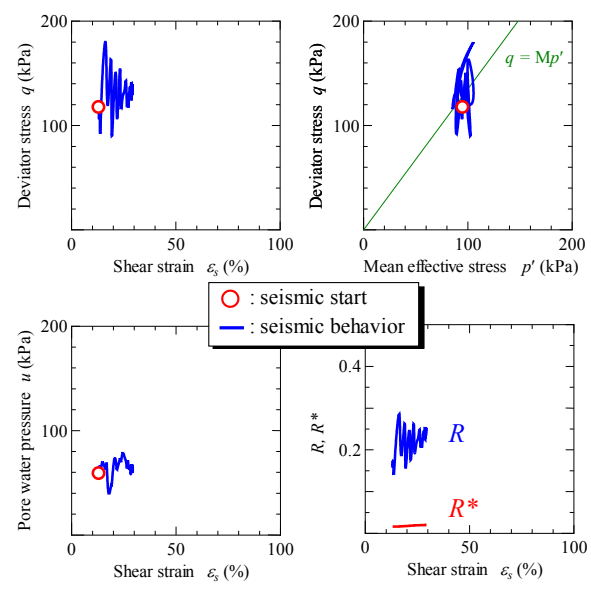


Figure 10. Behavior of the element at element-3 during Hyogo-ken Nanbu Earthquake

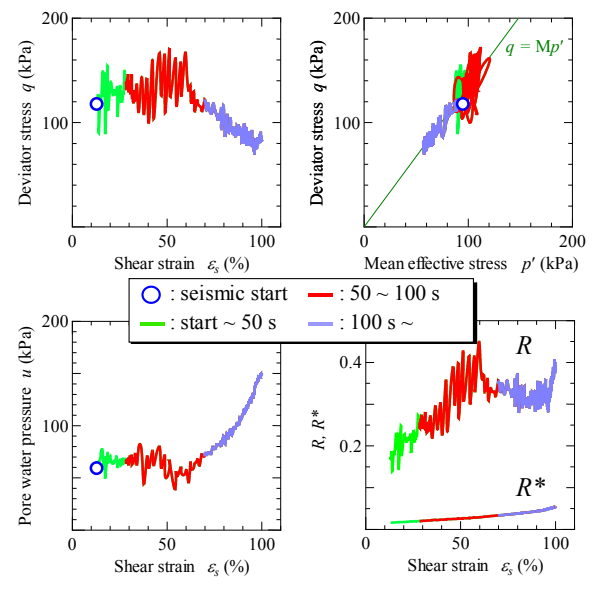


Figure 11. Behavior of the element at element-3 during the Great East Japan Earthquake

In both seismic waves, the progress of the shear strain at the toe of the slope was observed. However, the strain and deformation of the embankment differed greatly. To investigate it, the behavior of the element at the toe of the slope (element-3) during each earthquake was determined. Fig. 10 shows the behavior when data from the Hyogo-ken Nanbu Earthquake were input, and Fig. 11 shows the behavior when data from the Great East Japan Earthquake were input. In the Hyogo-ken Nanbu Earthquake, pore water pressure did not increase significantly and the mean effective stress did not decrease significantly. In addition, overconsolidation did not lose. While, in the Great East Japan Earthquake, the shear strain developed significantly in the

first and second acceleration groups. In particular, the second acceleration group had higher acceleration than the first acceleration group, so the strain was more advanced in the second acceleration group. Moreover, overconsolidation was lost, and the structure decayed compared with the Hyogo-ken Nanbu Earthquake. Then, the pore water pressure increased with plastic volume compression. As a result, the stiffness of the soil decreased, and the strain progressed, even if the amplitude of the seismic wave was small.

#### 6 CONCLUSIONS

In this study, a ground survey of an actual embankment was conducted, and a mechanical test of the collected samples was performed. Based on these results, the behavior of the mudstone embankment on the inclined ground during the seismic event was determined using *GEOASIA*. The conclusions are as follows.

- 1) The experimental results with the undisturbed sample could be reproduced when the triaxial compression test was calculated after simulating the sampling process using the material constants and the state of the element at the same point where the test was conducted. Therefore, the validity of the analysis code and the set material constants was confirmed.
- 2) When the seismic motion observed in the Great East Japan Earthquake was input, the shear strain at the toe of the slope developed remarkably. In addition, the mean effective stress in the embankment decreased due to the first and second acceleration groups. Because of decreasing mean effective stress, the stiffness of the soil decreased. Therefore, the shear strain further developed, even when the amplitude of the seismic wave was small. To the contrary, when the Hyogo-ken Nanbu Earthquake were input, no large deformation occurred because the seismic wave was short.
- 3) The survey revealed that slaking progresses not only between the observed highest groundwater level and the lowest groundwater level but also below the lowest groundwater level. The survey results show that the slaking ratio differed remarkably between the time of construction and the time of the ground survey. Thus, it is dangerous to use the slaking ratio as an index for material selection. Therefore, to understand the slaking property in detail, it is necessary to improve the tests, such as by increasing the number of times of drying and wetting.

## 7 REFERENCES

Asaoka, A., Noda, T., Yamada, E., Kaneda, K. and Nakano, M. 2 002. An elasto-plastic description of two distinct volume chan ge mechanisms of soils. Soils and Foundations 42 (5), 47-57.

Japan Road Association: https://www.road.or.jp/dl/tech.html. (Date viewed: 2019/12/10)

Nakano, M. and Sakai, T. 2016. Interpretation of slaking of a mudstone embankment using soil skeleton structure model concept and reproduction of embankment failure by seismic analysis. *Japanese Geotechnical Society Special Publication* 2 (5), 282-287.

Noda, T., Asaoka, A. and Nakano, M. 2008. Soil-water coupled finite deformation analysis based on a rate-type equation of motion incorporating the SYS Cam-clay model. *Soils and Foundations* 48 (6), 771-790.

Noda, T., Takeuchi, H., Nakai, K. and Asaoka, A. 2009. Co-seis mic and post seismic behavior of an alternately layered sand-c lay ground and embankment system accompanied by soil distu rbance. Soils and Foundations 49 (5), 739-756.

Sakai, T. and Nakano, M. 2019. Effects of slaking and degree of compaction on the mechanical properties of mudstones with varying slaking properties. Soils and Foundations 59 (1), 56-66.

Sharma, K., Kiyota, T. and Kyokawa, H. 2017. Effect of slaking on direct shear behaviour of crushed mudstones. *Soils and Foundations* 57 (2), 288-300